Global change in terrestrial ecosystem detected by fusion of microwave and optical satellite observations

Hideharu Nara[1] and Yohei Sawada[2]

[1]the University of Tokyo
[2]The University of Tokyo

November 22, 2022

Abstract

The detection and quantification of global land change by satellite observations are the grand challenges to improve the understanding of global environmental change. In this study, we develop a new vegetation index, which can be used as a proxy of the fractions of tree canopy and short vegetation, based on the simple linear regression between microwave vegetation optical depth (VOD) and optical leaf area index (LAI). Although we use no high-resolution reference data, the newly developed vegetation index successfully detects and quantifies the global land change which has been reported by the previous estimations based on high-resolution reference data. We find that the relationship between VOD and LAI is non-stationary and the temporal change in the VOD-LAI relationship is the important signal to detect and quantify global change in the terrestrial ecosystem.

Global change in terrestrial ecosystem detected by fusion of microwave and optical satellite observations

Running title: global land change by microwave and optical observations

Hideharu Nara[1+], Yohei Sawada[2+],

[1] Department of Civil Engineering, the University of Tokyo, Tokyo, Japan

[2] Institute of Engineering Innovation, the University of Tokyo, Tokyo, Japan

+These authors have equally contributed and should be considered as co-first authors.

manuscript to be submitted to *Geophysical Research Letters*

Corresponding author: Y. Sawada, Institute of Engineering Innovation, the University of Tokyo, Tokyo, Japan, 2-11-6, Yayoi, Bunkyo-ku, Tokyo, Japan, yohei.sawada@sogo.t.u-tokyo.ac.jp

Abstract

The detection and quantification of global land change by satellite observations are the grand challenges to improve the understanding of global environmental change. In this study, we develop a new vegetation index, which can be used as a proxy of the fractions of tree canopy and short vegetation, based on the simple linear regression between microwave vegetation optical depth (VOD) and optical leaf area index (LAI). Although we use no high-resolution reference data, the newly developed vegetation index successfully detects and quantifies the global land change which has been reported by the previous estimations based on high-resolution reference data. We find that the relationship between VOD and LAI is non-stationary and the temporal change in the VOD-LAI relationship is the important signal to detect and quantify global change in the terrestrial ecosystem.

Plain language summary

The detection and quantification of global land change, such as deforestation and afforestation, are crucially important to understand the effects of climate change and human activities on the terrestrial ecosystem. There are two major methodologies of satellite remote sensing of vegetation: optical and microwave remote sensing. While

photosynthetic activities of plants can be observed by optical remote sensing, total aboveground vegetation water content can be observed by microwave remote sensing. Here we find that the simple linear regression between two vegetation indices generated from optical and microwave satellite observations can accurately quantify the fractions of tree canopy and short vegetation in the observation pixels. We apply this finding to detect global land change from 2003 to 2019. We can detect several important land changes, such as tree canopy gain in Sahel and deforestation in southeastern Amazon.

Key Points

1. The simple linear regression between VOD and LAI can quantify the fractions of tree canopy and short vegetation/bare ground.

2. The relationship between VOD and LAI is non-stationary and its temporal change is the important signal to detect global land change.

1. Introduction

The detection and quantification of global change in the terrestrial ecosystem are crucially important to understand global environmental change. Vegetation indices generated from optical satellite observations (e.g., Zhu et al. 2013; Tucker et al. 2005) have been intensively used to monitor the change in the terrestrial ecosystem. For example, Song et al. (2018) developed a yearly global vegetation product, in which every land pixel is characterized by its per cent cover of tree canopy, short vegetation, and bare ground, from the optical-infrared Normalized Difference Vegetation Index (NDVI), and successfully detected the long-term global land change.

The limitation of the optical satellite observation is that it is sensitive only to a photosynthetically active part of terrestrial biomass (i.e. leaf) and it is not straightforward to retrieve the amount of a photosynthetically inactive part of aboveground biomass (i.e. woody biomass). To distinguish tree canopy and short vegetation from optical satellite observations, complex supervised machine learning with high-resolution reference data is usually required (e.g., Song et al. 2018). To overcome this limitation, microwave remote sensing has been recognized as an alternative approach to monitor global change in the terrestrial ecosystem. Microwave Vegetation Optical Depth (VOD) is sensitive to vegetation water content, which includes the information of both leaf and woody biomass (see Owe et al. (2001) and Jones et al. (2011) for the detailed description of VOD and the retrieval algorithms). Liu et al. (2015) successfully monitored the long-term change in global aboveground biomass carbon by microwave VOD data. Zhou et al. (2014) indicated that microwave VOD was more sensitive to the degradation of the Congo rainforest by drought than the optical vegetation index.

Combining the microwave and optical vegetation indices has the potential to improve the understanding of vegetation dynamics. Jones et al. (2013) found that the post-fire recovery of NDVI was much faster than that of microwave VOD, which indicated the faster recovery of short vegetation than woody biomass after extreme wildfires in Alaska and Canada. Van Dijk et al. (2013) found that in the Australian millennium drought, no decreasing trend could be detected in the optical vegetation indices while microwave VOD significantly declined. By numerical simulation, Sawada and Koike (2016) attributed this difference to the higher resilience of short vegetation to drought than woody biomass. These studies showed the high potential of fusions of microwave and optical satellite observations to distinguish the dynamics of tree canopy and short vegetation.

We aim to develop a new method to detect global land change by combining microwave VOD and optical Leaf Area Index (LAI). We reveal that the simple linear regression between microwave VOD and optical LAI provides a useful proxy of the fractions of tree canopy and short vegetation. The proposed vegetation index successfully detects and quantifies global change in the terrestrial ecosystem from 2003 to 2019 without any additional reference data.

2. Data

We used the microwave VOD product based on the Land Parameter Retrieval Model (LPRM) provided by National Aeronautics and Space Administration (NASA). The description of the LPRM algorithm can be found in Owe et al. (2001) and Owe et al. (2008). Microwave VOD is retrieved from C-band (6.9 GHz) brightness temperature observed by Advanced Microwave Scanning Radiometer for Earth observation system (AMSR-E) and AMSR2. The VOD products from both AMSR-E (from June 2002 to September 2011) and AMSR2 (from July 2012 to December 2019) were used. We used only night scene data to reduce the effect of a surface temperature bias in the retrieval algorithm (Liu et al. 2011). The spatial resolution of this dataset is 0.25 degree. The temporal resolution of this dataset is approximately 2-daily, and we resampled it to 8-daily.

We used the optical LAI product processed by Ichii et al. (2017). Ichii et al. (2017) applied detailed quality control to MODerate resolution Imaging Spectroradiometer (MODIS) onboard Terra and Aqua satellites LAI L4 data (MCD15A2H; Myneni et al. 2015). The spatial and temporal resolutions are 0.25 degree and 8-daily, respectively.

As land cover data, we used the MODIS land cover climate modeling grid (MCD12C1) version 6 data product (Friedl et al. 2015). The temporal resolution of this dataset is yearly. The original spatial resolution of this dataset is 0.05 degree and we resampled it to 0.25 degree by the nearest neighbor approach.

3. Method

The Microwave and Optical Fusion Approach (MiOFA) was originally proposed by Sawada et al. (2017a) to improve the skill to retrieve surface soil moisture and vegetation water content from C-band brightness temperature. In the MiOFA, the relationship between VOD and total aboveground Vegetation Water Content (VWC) can be formulated as:

$$VOD = b \times VWC + R \quad (1)$$

where b is a parameter and R quantifies the effect of surface soil roughness. Because it is difficult to distinguish the effects of vegetation and surface soil roughness on brightness temperature, the existing VOD data include the effect of surface soil roughness (e.g., Sawada et al. 2016, 2017a, 2017b; Wang et al. 2015; Njoku and Chan 2006). The important assumption of the MiOFA is that b-parameter for C-band VOD is time-invariant and species-independent. Sawada et al. (2016) and Sawada et al. (2017b) supported this assumption by a field experiment although Jackson and Schmugge (1991) originally formulated this parameter as a species-dependent variable.

Paloscia and Pampaloni (1988) proposed the empirical relationship between VWC and optical LAI, which was supported by the in-situ observations (e.g., Sawada et al. 2017b):

$$VWC = \exp\left(\frac{LAI}{y}\right) - 1 \cong \frac{LAI}{y} \quad (2)$$

where y is a species-dependent parameter which cannot be directly observed by satellite sensors. The y-parameter can be recognized as the contribution of leaf biomass to the total aboveground VWC. The lower y indicates the larger fraction of short vegetation since the small increase of LAI induces the large increase of total aboveground VWC. The higher y indicates that there is the larger amount of tree canopy. The y-parameter can be a good index of canopy biomass structure.

By substituting (2) to (1), we obtain the equation (3).

$$VOD = \frac{b}{y} LAI + R \quad (3)$$

The MiOFA proposes to estimate the parameters of canopy biomass structure (b/y) and surface soil roughness (R) by the linear regression between microwave VOD and optical LAI. In the original paper of the MiOFA (Sawada et al. 2017a), the R-parameter was focused on to improve the retrieval of surface soil moisture. In this paper, we focused on the slope of the linear regression, b/y, as a vegetation index. Because we assumed that b is a constant parameter, we hypothesized that tree canopy (short vegetation) is dominant in pixels with lower (higher) b/y.

By performing the linear regression between microwave VOD and optical LAI, we developed the yearly global b/y dataset from 2003 to 2019. Since we had no C-band brightness temperature observations in the transition period from AMSR-E to AMSR2, we did not estimate b/y in 2011 and 2012 (see also section 2). There are long-term and temporally continuous VOD datasets derived by merging the multi-sensor VOD products (e.g., Moesinger et al. 2020). However, the assumption of the constant b-parameter is correct only in the lower frequencies such as C-band so that we avoided to use VOD retrieved by brightness temperature with higher frequencies in this first application. No significant inconsistency between AMSR-E and AMSR2 has been found in the previous calibration studies (e.g., Okuyama and Imaoka 2015; Parinussa et al.

2015; Du et al. 2017). We showed b/y in the pixels where the slope of the linear regression is positive and statistically significant with a 95% confidence level.

4. Results and discussion

Figure 1 shows climatologic b/y from 2003 to 2019. We use all 8-daily data of microwave VOD and optical LAI in the study period to perform the linear regression, and the estimated slope is shown in Figure 1. Although the linear relationship between microwave VOD and optical LAI is statistically insignificant in the rainforest regions due to the saturation of the signals of VOD and/or LAI in the densely vegetated areas, we can retrieve b/y in most of the vegetated pixels. Generally, b/y tends to be low in the temperate and boreal forest areas. In semiarid grassland, b/y is relatively high indicating the large contribution of LAI to VWC. The spatial distribution of the retrieved R-parameter shown in Figure S1 is similar to the previous global estimation of a roughness parameter in a radiative transfer model (Wang et al. 2015).

To confirm that b/y can be used as the proxy of the fractions of tree canopy and short vegetation, we estimated yearly b/y and compared it with the yearly land cover type data. Figures 2 and S2 indicate that we obtain low b/y in broadleaf and needleleaf forest areas. b/y increases in savannas, cropland, and grassland areas. In pixels with lower (higher) b/y, tree canopy (short vegetation) is dominant so that our proposed b/y can be a useful index to quantify the fractions of tree canopy and short vegetation. It is not straightforward to distinguish tree canopy dominant pixels from short vegetation dominant pixels by simply analyzing yearly optical LAI (Figure S3). Boxplots in Figure 2 show the large variance of b/y in the specific land cover types probably due to the coarse resolution of microwave VOD, which prevents the direct matchup of b/y with the land cover data (see also section 2).

We can detect global land change by our yearly b/y. Figure 3 shows the linear trend of yearly b/y from 2003 to 2019. The decrease of b/y (shown in blue) indicates the increase of tree canopy, and the increase of b/y (shown in red) indicates the increase of short vegetation/bare ground. Most of the detected trends are consistent to the previous findings. We can detect the increase of tree canopy in the Sahel region, which previous studies attributed to the increase of rainfall (Brandt et al. 2017: Hickler et al. 2005). The increase of tree canopy in eastern Europe detected in our dataset is consistent to previous studies (e.g., Potapov et al. 2015; Hansen et al. 2013). We can detect the widespread increase of tree canopy in China, which resulted from reforestation and afforestation programs (e.g., Piao et al. 2015). The decreasing trend of b/y is also detected in western India, which can be attributed to the transition from bare ground to short vegetation by agricultural activities (Tian et al. 2014). The decrease of tree canopy in southeastern Amazon and Siberia detected in our dataset is also consistent to the previous findings (e.g., Hansen et al. 2013).

The global land change detected by our newly developed b/y index is consistent to the state-of-the-art dataset provided by Song et al. (2018). Song et al. (2018) estimated the long-term trend of the fractions of tree canopy, short vegetation, and bare ground from NDVI by supervised machine learning with high-resolution reference data. It is promising that our proposed method can detect the similar change in the terrestrial ecosystem to Song et al. (2018) by the simple linear regression between microwave VOD and optical LAI without any reference data. However, there are some differences between changes detected by this study and Song et al. (2018). Song et al. (2018) detected the short vegetation gain in the Congo rainforest, which we do not detect. Song et al. (2018) detected the tree canopy gain in eastern U.S. while the long-term trend in this region is unclear in our dataset. Our estimated trend in Siberia is also inconsistent to

Song et al. (2018) although it is consistent to the other estimation which focused only on forest cover (Hansen et al. 2013). There are several reasons for these differences. First, the linear regression between microwave VOD and optical LAI is insignificant in densely vegetated areas as shown in Figure 1 so that our b/y index cannot accurately quantify vegetation dynamics in the dense rainforest. Second, the study period in this study (2003-2019) is different from that in Song et al. (2018) (1982-2016). The human influence on the terrestrial ecosystem in the 20^{th} century cannot be detected in our dataset. Third, the spatial resolution of our b/y data (0.25 degree) is much lower than that of Song et al. (2018) (0.05 degree) so that many impacts of human activities on vegetation dynamics in small scales may be invisible in our data.

The results shown above imply that the empirical equations and assumptions of the MiOFA described in section 3 are accurate in the global scale. Since these empirical equations and assumptions are closely related to the algorithms to retrieve surface soil moisture and VOD from brightness temperature (e.g., Owe et al. 2001, 2008; Fujii et al. 2009; Sawada et al. 2017a) and to assimilate brightness temperature into land surface models (e.g., Yang et al. 2007, 2009; Sawada and Koike 2014; Sawada et al. 2015), our retrieved b/y and R parameters may greatly contribute to improving these algorithms and the understanding of microwave radiative transfer in the canopy. The most important implication of this study is that the relationship between microwave VOD (or VWC) and the optical vegetation index is non-stationary although it is assumed to be stationary in previous studies on the development and validation of the VWC retrieval algorithms (e.g., Gao et al. 2015). The temporal change in the VOD-LAI relationship is the important signal to quantify global environmental change so that it should not be neglected in the development, validation, and analysis of satellite land observation products.

5. Conclusions

We propose the new vegetation index by combining microwave VOD and optical LAI. Our new index can be the good proxy of the fractions of tree canopy and short vegetation and is useful to detect and quantify global change in the terrestrial ecosystem. The advantage of our new method is that the vegetation index can be obtained by the simple linear regression between microwave VOD and optical LAI so that no high-resolution reference data are required. The limitation is the lower spatial resolution than the other existing methods. Future work will focus on the applications of this new vegetation index to deepen the understanding of vegetation dynamics in extreme climate conditions such as drought.

Acknowledgement

YS designed the study. HN performed the analysis. HN and YS jointly interpreted the results. YS wrote the first draft of the paper and HN contributed to editing it. This study was supported by JAXA grant ER2GWF102 and JSPS KAKENHI grant 18H03800. The microwave VOD data can be downloaded at https://disc.gsfc.nasa.gov/datasets/LPRM_AMSR2_A_SOILM3_001/summary. The optical LAI data can be downloaded at ftp://modis.cr.chiba-u.ac.jp/ichii/DATA/MODIS/. The land cover data can be downloaded at https://lpdaac.usgs.gov/products/mcd12c1v006/.

References

Brandt, M., et al. (2017), Human population growth offsets climate-driven increase in woody vegetation in sub-Saharan Africa., *Nature Ecology & Evolution, 1*, 0081, https://doi.org/10.1038/s41559-017-0081

Du, J., Kimball, J. S., Jones, L. A., Kim, Y., Glassy, J., & Watts, J. D. (2017), A global satellite environment data record derived from AMSR-E and AMSR2 microwave

Earth observations, *Earth System Science Data, 9,* 791-808, https://doi.org/10.5194/essd-9-791-2017.

Friedl, M. & Sulla-Menashe, D. (2015), MCD12C1 MODIS/Terra+Aqua Land Cover Type Yearly L3 Global 0.05Deg CMG V006. distributed by NASA EOSDIS Land Processes DAAC, https://doi.org/10.5067/MODIS/MCD12C1.006.

Fujii, H., Koike, T., & Imaoka, K. (2009). Improvement of the AMSR-E algorithm for soil moisture estimation by introducing a fractional vegetation coverage dataset derived from MODIS data., *Journal of the Remote Sensing Society of Japan, 29*, 282-292., https://doi.org/10.11440/rssj.29.282

Gao, Y., Walker, J. P., Allahmoradi, M., Monerris, A., Ryu, D., & Jackson, T. J. (2015), Optical Sensing of Vegetation Water Content : A Synthesis Study, *IEEE Journal of Selected Topics in Applied Earth Observations and Remote Sensing, 8*, 1456-1464, https://doi.org/10.1109/JSTARS.2015.2398034.

Hansen, M. C. et al. (2013), High-Resolution Global Maps of 21st-Century Forest Cover Change, *Science, 342,* 850-853, https://doi.org/10.1126/science.1244693.

Hickler, T., Eklundh, L., Seaquist, J. W., Smith, B., Ardö, J., Olsoon, L., Sykes, M. T., and Sjöström, M. (2005), Precipitation controls Sahel greening trend, *Geophysical Research Letters, 32*, L21415, doi:10.1029/2005GL024370.

Ichii, K., et al. (2017), New data-driven estimation of terrestrial CO_2 fluxes in Asia using a standardized database of eddy covariance measurements, remote sensing data, and support vector regression, *Journal of Geophysical Research Biogeosciences.*, 122, 767– 795, doi:10.1002/2016JG003640.

Jackson, T. J., & Schmugge, T. J. (1991). Vegetation effects on the microwave emission of soils. *Remote Sensing of Environment, 36(3)*, 203–212. https://doi.org/10.1016/0034-4257(91)90057-D

Jones, M. O., Jones, L. a., Kimball, J. S., & McDonald, K. C. (2011). Satellite passive microwave remote sensing for monitoring global land surface phenology. *Remote Sensing of Environment*, *115*(4), 1102–1114. https://doi.org/10.1016/j.rse.2010.12.015

Jones, M. O., Kimball, J. S., & Jones, L. A. (2013). Satellite microwave detection of boreal forest recovery from the extreme 2004 wildfires in Alaska and Canada, *Global Change Biology, 19(10)*, 3111–3122. https://doi.org/10.1111/gcb.12288

Liu, Y. Y., De Jeu, R. a M., McCabe, M. F., Evans, J. P., & Van Dijk, A. I. J. M. (2011). Global long-term passive microwave satellite-based retrievals of vegetation optical depth. *Geophysical Research Letters*, *38*(18), 1–6. https://doi.org/10.1029/2011GL048684

Liu, Y. Y., van Dijk, A. I. J. M., de Jeu, R. a. M., Canadell, J. G., McCabe, M. F., Evans, J. P., & Wang, G. (2015). Recent reversal in loss of global terrestrial biomass. *Nature Climate Change*, *5*, 470–474, https://doi.org/10.1038/nclimate2581

Moesinger, L., Dorigo, W., de Jeu, R., van der Schalie, R., Scanlon, T., Teubner, I., & Forkel, M. (2020), The global long-term microwave Vegetation Optical Depth Climate Archive (VODCA), *Earth System Science Data, 12,* 177-196, https://doi.org/10.5194/essd-12-177-2020

Myneni, R., Knyazikhin, Y. & Park T. (2015), MOD15A2H MODIS/Terra Leaf Area Index/FPAR 8-Day L4 Global 500m SIN Grid V006. distributed by NASA EOSDIS Land Processes DAAC, https://doi.org/10.5067/MODIS/MOD15A2H.006.

Njoku, E. G., & Chan, S. K. (2006). Vegetation and surface roughness effects on AMSR-E land observations, *Remote Sensing of Environment, 100(2)*, 190–199. https://doi.org/10.1016/j.rse.2005.10.017

Okuyama, A. & Imaoka, K. (2015), Intercalibration of Advanced Microwave Scanning Radiometer-2 (AMSR2) Brightness Temperature, *IEEE Transactions on Geoscience and Remote Sensing*, *53,* 4568-4577, https://doi.org/10.1109/TGRS.2015.2402204

Owe, M., De Jeu, R., & Walker, J. (2001). A methodology for surface soil moisture and vegetation optical depth retrieval using the microwave polarization difference index. *IEEE Transactions on Geoscience and Remote Sensing*, *39*(8), 1643–1654. https://doi.org/10.1109/36.942542

Owe, M., de Jeu, R., & Holmes, T. (2008). Multisensor historical climatology of satellite-derived global land surface moisture. *Journal of Geophysical Research: Earth Surface*, *113*(1), 1–17. https://doi.org/10.1029/2007JF000769

Paloscia, S., & Pampaloni, P. (1988). Microwave polarization index for monitoring vegetation growth. *IEEE Transactions on Geoscience and Remote Sensing, 26(5)*, 617–621. https://doi.org/10.1109/36.7687

Parinussa, R. M., Holmes, T. R. H., Wanders, N., Dorigo, W. A., & de Jeu, R. A. M. (2015) A Preliminary Study toward Consistent Soil Moisture from AMSR2. *Journal of Hydrometeorology*, *16*, 932–947, https://doi.org/10.1175/JHM-D-13-0200.1.

Piao, S., et al. (2015), Detection and attribution of vegetation greening trend in China over the last 30 years. *Global Change Biology, 21,* 1601-1609. https://doi.org/10.1111/gcb.12795

Potapov, P. V., Turubanova, S. A., Tyukavina, A., Krylov, A. M., McCarty, J. L., Radeloff, V. C. & Hansen, M. C. (2015), Eastern Europe's forest cover dynamics from 1985 to 2012 quantified from the full Landsat archive, *Remote Sensing of Environment, 159,* 28-43, https://doi.org/10.1016/j.rse.2014.11.027.

Sawada, Y., & Koike, T. (2014). Simultaneous estimation of both hydrological and ecological parameters in an ecohydrological model by assimilating microwave signal., *Journal of Geophysical Research, 119*, 8839-8857, https://doi.org/10.1002/2014JD021536

Sawada, Y., Koike, T., & Walker, J. P. (2015). A land data assimilation system for simultaneous simulation of soil moisture and vegetation dynamics. *Journal of Geophysical Research, 120*, 5910-5930, https://doi.org/10.1002/2014JD022895

Sawada, Y. & Koike, T. (2016), Ecosystem resilience to the Millennium drought in southeast Australia (2001–2009), *Journal of Geophysical Research Biogeosciences*, *121*, 2312– 2327, doi:10.1002/2016JG003356.

Sawada, Y., Tsutsui, H., Koike, T., Rasmy, M., Seto, R., & Fujii, H. (2016). A field verification of an algorithm for retrieving vegetation water content from passive microwave observations. *IEEE Transactions on Geoscience and Remote Sensing, 54(4),* 2082-2095, https://doi.org/10.1109/TGRS.2015.2495365

Sawada, Y., Koike, T., Aida, K., Toride, K., & Walker, J. P. (2017a). Fusing Microwave and Optical Satellite Observations to Simultaneously Retrieve Surface Soil Moisture, Vegetation Water Content, and Surface Soil Roughness. *IEEE Transactions on Geoscience and Remote Sensing*, *55*(11), 6195-6206, https://doi.org/10.1109/TGRS.2017.2722468

Sawada, Y., Tsutsui, H., & Koike, T. (2017b), Ground Truth of Passive Microwave Radiative Transfer on Vegetated Land Surfaces. *Remote Sensing., 9,* 655, https://doi.org/10.3390/rs9070655

Song, X.-P., Hansen, M. C., Stehman, S. V., Potapov, P. V., Tyukavina, A., Vermote, E. F., & Townshend, J. R. (2018). Global land change from 1982 to 2016. *Nature*, *560,* 639-643, https://doi.org/10.1038/s41586-018-0411-9

Tian, H., Banger, K., Bo, T., Dadhwal, V. K. (2014), History of land use in India during 1880–2010: Large-scale land transformations reconstructed from satellite data and historical archives, *Global and Planetary Change, 121,* 78-88, https://doi.org/10.1016/j.gloplacha.2014.07.005

Tucker, C. J. et al. (2005), An extended AVHRR 8 - km NDVI dataset compatible with MODIS and SPOT vegetation NDVI data, *International Journal of Remote Sensing, 26,* 4485-4498, https://doi.org/10.1080/01431160500168686

Van Dijk, A. I. J. M., et al. (2013). The Millennium Drought in southeast Australia (2001-2009): Natural and human causes and implications for water resources, ecosystems, economy, and society. *Water Resources Research*, *49*(2), 1040–1057. https://doi.org/10.1002/wrcr.20123

Wang, S., et al. (2015), Global-Scale Evaluation of Roughness Effects on C-Band AMSR-E Observations. *Remote Sensing, 7(5),* 5734–5757. https://doi.org/10.3390/rs70505734

Yang, K., Watanabe, T., Koike, T., Li, X., Fujii, H., Tamagawa, K., Ma, Y. & Ishikawa, H. (2007), Auto-calibration System Developed to Assimilate AMSR-E Data into a Land Surface Model for Estimating Soil Moisture and the Surface Energy Budget, *Journal of the Meteorological Society of Japan, 85A,* 229–242. https://doi.org/10.2151/jmsj.85A.229

Yang, K., Koike, T., Kaihotsu, I., & Qin, J. (2009). Validation of a Dual-Pass Microwave Land Data Assimilation System for Estimating Surface Soil Moisture in Semiarid Regions., *Journal of Hydrometeorology, 10(3)*, 780–793. https://doi.org/10.1175/2008JHM1065.1

Zhou, L., et al. (2014). Widespread decline of Congo rainforest greenness in the past decade. *Nature*, *509*(7498), 86–90. https://doi.org/10.1038/nature13265

Zhu, Z. et al. (2013), Global Data Sets of Vegetation Leaf Area Index (LAI)3g and Fraction of Photosynthetically Active Radiation (FPAR)3g Derived from Global Inventory Modeling and Mapping Studies (GIMMS) Normalized Difference Vegetation Index (NDVI3g) for the Period 1981 to 2011., *Remote Sensing, 5,* 927-948, https://doi.org/10.3390/rs5020927.

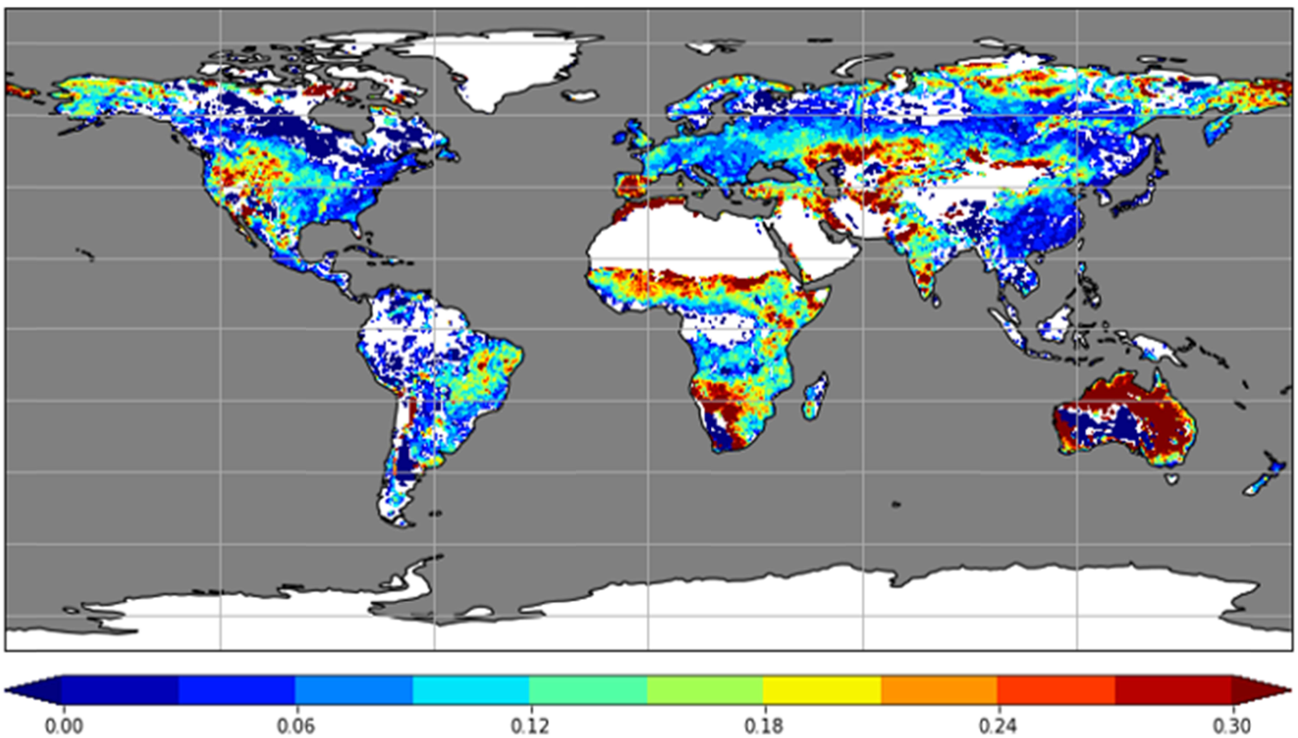

Figure 1. Climatologic b/y [-] (see section 3). Pixels which show a statistically significant slope between microwave VOD and optical LAI (student's t-test, $p<0.05$) are depicted.

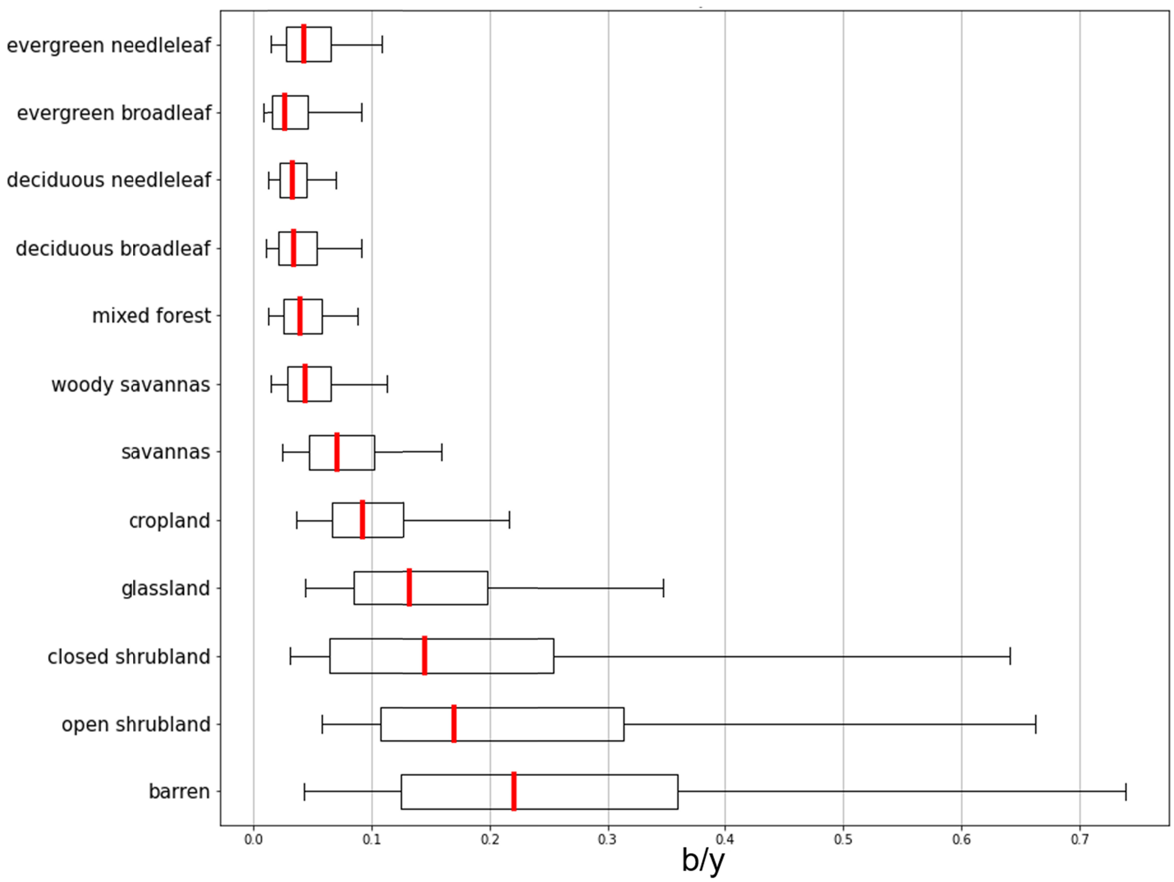

Figure 2. Boxplots of yearly b/y [-] (see section 3) stratified by land cover types. Pixels of water, wetland, urban, mosaic, and ice are excluded.

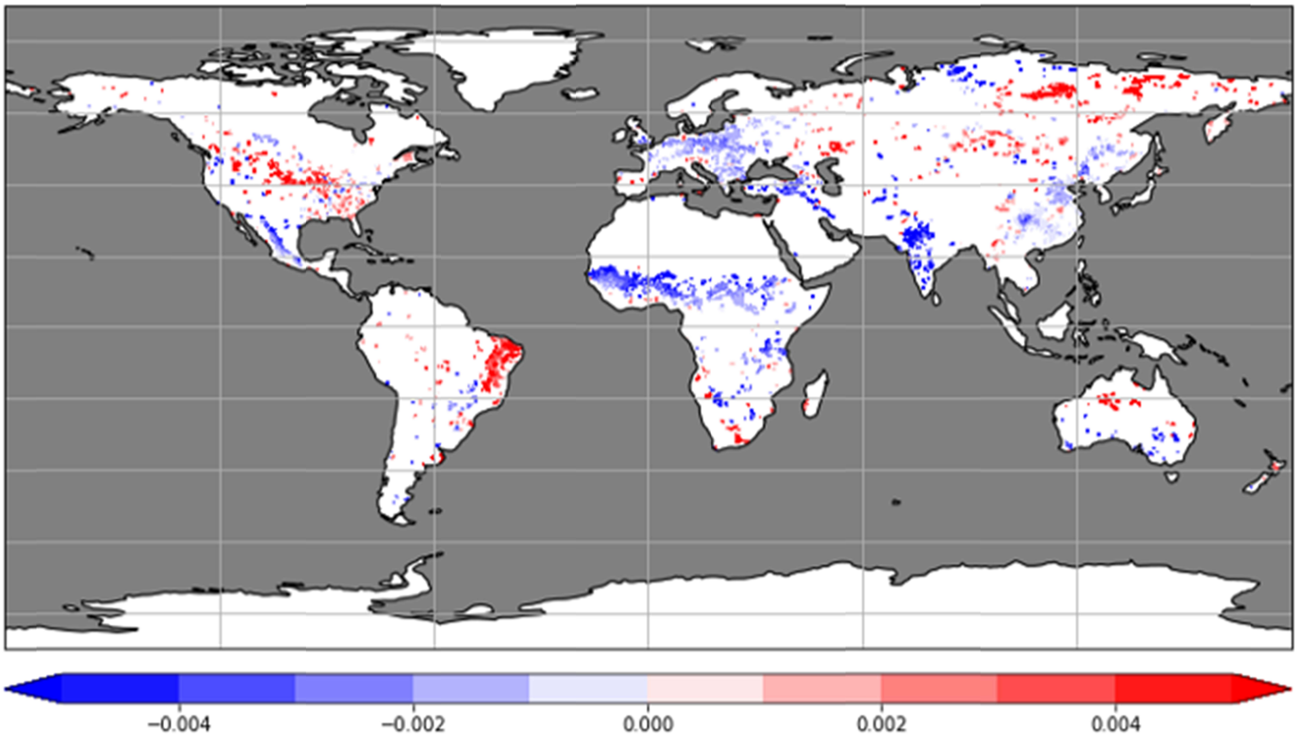

Figure 3. Linear trend of b/y [-] (see section 3) from 2003 to 2019. Pixels which show a statistically significant trend (student's t-test, $p<0.05$) are depicted.